Three-dimensional fractal modeling of intracloud lightning discharge in a New Mexico thunderstorm and comparison with lightning mapping observations

Jeremy A. Riousset,[1] Victor P. Pasko,[1] Paul R. Krehbiel,[2] Ronald J. Thomas,[3] and William Rison[3]

Received 5 June 2006; revised 27 March 2007; accepted 9 May 2007; published 4 August 2007.

[1] The direct comparison of lightning mapping observations by the New Mexico Tech Lightning Mapping Array (LMA) with realistic models of thundercloud electrical structures and lightning discharges represents a useful tool for studies of electrification mechanisms in thunderstorms, initiation and propagation mechanisms of different types of lightning discharges as well as for understanding of electrical and energetic effects of tropospheric thunderstorms on the upper regions of the Earth's atmosphere. This paper presents the formulation of a new three-dimensional probabilistic model for investigating the structure and development of bidirectional positive and negative lightning leaders. The results closely resemble structures observed by the LMA during intracloud discharges. The model represents a synthesis of the original dielectric breakdown model based on fractal approach proposed by Niemeyer et al. (1984) and the equipotential lightning channel hypothesis advanced by Kasemir (1960) and places special emphasis on obtaining self-consistent solutions preserving complete charge neutrality of the discharge trees at any stage of the simulation. A representative simulation run is compared to a typical intracloud discharge measured by LMA in a New Mexico thunderstorm on 31 July 1999. Following the conclusions from Coleman et al. (2003), the comparison of the model and observed discharges reveals that an adequate choice of the electrical structure of the model thundercloud permits the development of a model intracloud discharge reproducing principal features of the observed event including the initial vertical extension of the discharge between the main negative and upper positive charge regions of the thundercloud, and the subsequent horizontal propagations in these regions. Also consistent with observations (e.g., Coleman et al., 2003), negative and positive leaders mainly develop in the upper positive and main negative charge regions, respectively. For the particular model case presented in this paper, the total charge transfer, the vertical dipole moment and the average linear charge density associated with the development of bidirectional structure of leader channels are estimated to be 37.5 C, 122 C·km, and 0.5 mC/m, respectively, in good agreement with related data reported in the refereed literature. The model results also demonstrate that the bulk charge carried by the integral action of positive and negative leaders leads to a significant (up to 80%) reduction of the electric field values inside the thundercloud, significantly below the lightning initiation threshold.

Citation: Riousset, J. A., V. P. Pasko, P. R. Krehbiel, R. J. Thomas, and W. Rison (2007), Three-dimensional fractal modeling of intracloud lightning discharge in a New Mexico thunderstorm and comparison with lightning mapping observations, *J. Geophys. Res.*, *112*, D15203, doi:10.1029/2006JD007621.

1. Introduction

[2] The leader process as a propagation mechanism of cloud-to-ground lightning was determined photographically as early as the 1930s by Schonland, Malan and coworkers in South Africa (as summarized by *Uman* [1984, p. 5; 2001, pp. 7 and 83]). This basic mechanism is now known to be also valid for intracloud discharges [*Ogawa and Brook*, 1964; *Proctor*, 1981, 1983; *Uman*, 1984, p. 10; *Liu and Krehbiel*, 1985; *Shao and Krehbiel*, 1996; *Rakov and*

[1]Communications and Space Sciences Laboratory, Department of Electrical Engineering, Pennsylvania State University, University Park, Pennsylvania, USA.
[2]Physics Department, New Mexico Institute of Mining and Technology, Socorro, New Mexico, USA.
[3]Electrical Engineering Department, New Mexico Institute of Mining and Technology, Socorro, New Mexico, USA.

0148-0227/07/2006JD007621

Uman, 2003, p. 322]. However, understanding of the internal physics of the leader process is still far from complete [e.g., *Bazelyan and Raizer*, 2000, pp. 84–85; *Gallimberti et al.*, 2002; *Pasko*, 2006, and references therein]. The complexity of the phenomenon and the lack of a complete theory on lightning propagation led some authors to consider only the bulk effects of the lightning discharges in the development of cloud electrification models [e.g., *Ziegler and MacGorman*, 1994; *Krehbiel et al.*, 2004]. The model presented in this paper continues a long-lasting effort started in the 1950s directed toward a theoretical description of the interaction between the lightning channel and the surrounding thunderstorm electric field [e.g., *Kasemir*, 1960, and references therein].

[3] *Kasemir* [1960] modeled the lightning channel as an equipotential, overall neutral, prolonged spheroid placed in the thundercloud electric field. The spheroid is vertical and lies on the main axis of the system, which is assumed to possess a rotational symmetry. The induced linear charge density on the channel is derived on the basis of the surrounding ambient potential of the thundercloud. *Mazur and Ruhnke* [1998] revisited *Kasemir*'s [1960] model with the same assumptions of overall neutrality and equipotentiality in order to investigate the relationships among cloud charges, potentials and electric fields, and the induced charges, currents, and electric field changes associated with the lightning channel. The linear charge density in the channel was no longer derived analytically on the basis of the assumption of spheroid channel but determined numerically to account for the geometry of the channel used in their model. This work utilized a tripolar-like charge model to study the development of cloud-to-ground and intracloud discharges, but the system remained axisymmetric and did not allow for branching or horizontal development. Unlike *Kasemir*'s [1960] model, in which the estimation of the potential was done for a channel of fixed length, *Mazur and Ruhnke* [1998] introduced a dynamical variation of the channel length to simulate the discharge progression.

[4] In their three-dimensional simulations of electric fields within a thunderstorm, *Hager et al.* [1989] introduced a deterministic lightning model, which allowed branching of the discharge channels. In this model, whenever some component of the electric field reaches a predefined breakdown threshold, the conductivity between the corresponding mesh points is taken to infinity. As the conductivity tends to infinity, the potential is adjusted throughout the domain, so that in the breakdown region, the potential is constant. This adjustment to the potential, which does not account for the overall neutrality of the discharge, often leads to cascades; in the process of equilibrating the potential between two nodes, the electric field between an adjacent pair of nodes reaches the breakdown threshold [*Hager et al.*, 1989].

[5] Recently, *Behnke et al.* [2005] applied the principles of *Mazur and Ruhnke*'s [1998] model to investigate the evolution of initial leader velocities during intracloud lightning. Instead of *Mazur and Ruhnke*'s [1998] model of a thundercloud, the authors used a more realistic model derived from lightning mapping and electric field sounding observations of actual storms. Like *Mazur and Ruhnke* [1998], *Behnke et al.* [2005] ensured the overall neutrality of the channel by adequately shifting the electric potential of the channel.

[6] *Helsdon et al.* [1992] used *Kasemir*'s [1960] equipotential, spheroid, overall neutral representation of the lightning in their Storm Electrification Model. The problem was solved in a two-dimensional (2-D) Cartesian domain, with no hypothesis concerning the symmetry of the channel. To overcome the difficulty of deriving a linear charge density in 2-D, *Helsdon et al.* [1992] derived an analytical expression for the linear charge density carried by a channel of the designated spheroid geometry. In this model, the lightning propagates with no branching along the field lines defined by the ambient field configuration regardless of the electric field due to the lightning channel itself. *Helsdon et al.* [2002] extended the previous model to a 3-D geometry. The channel is again neutral and equipotential and propagates bidirectionally between the grid points of the three-dimensional Cartesian space, with essentially the same limitations as in the 1992 model. Other models based on the same concepts have been developed but are not described here for the sake of brevity. A review of those is given by *Poeppel* [2005, pp. 1–5].

[7] A significant limitation of the aforementioned models is related to the deterministic character of the lightning propagation. Indeed, none of these models is able to reproduce the observed morphology of highly distorted and branched path of the lightning in a realistic way. This issue cannot be resolved at present using a microscopic approach to the lightning propagation because of insufficient knowledge of the related processes and also because of the lack of computational power. Instead, *Petrov and Petrova* [1993] used *Niemeyer et al.*'s [1984] Dielectric Breakdown Model to introduce stochasticity in the modeling of the lightning discharge. The original model by *Niemeyer et al.* [1984] has been further discussed, refined and improved by *Satpathy* [1986], *Niemeyer et al.* [1986], *Wiesmann and Zeller* [1986], *Niemeyer and Wiesmann* [1987], *Niemeyer et al.* [1989], and *Femia et al.* [1993]. The idea of these models is to simulate the observed macroscopic behavior of the leader by using a probabilistic approach rather than by describing its internal physics. Such models have been successfully applied to reproduce other atmospheric phenomena such as sprites [e.g., *Pasko et al.*, 2000, 2001]. *Petrov and Petrova*'s [1993] model used a dipole electrode representation of a thundercloud in a 2-D Cartesian space. The links between grid points resembling lightning channels were initiated from a central circular region in the simulation domain where the potential was kept constant. The model used unusually high electric field values for the discharge initiation threshold and employed a variable voltage drop along the channel to simulate its resistivity. *Petrov et al.* [2003] further extended this model to a 3-D Cartesian geometry to predict the probability of lightning strikes to practical structures. As in their previous model, the potential of a point of a new link at the moment of its connection with the discharge remained unchanged for the remainder of the simulation. No assumptions concerning the channel neutrality were employed and no charge densities were derived.

[8] *Mansell et al.* [2002] also extended *Niemeyer et al.*'s [1984] model to a 3-D Cartesian geometry. In addition, they added bidirectional propagation of the model lightning

trees, and integrated it in a numerical thunderstorm model. As in the work by *Petrov and Petrova* [1993], the channel is resistive but with a fixed voltage drop between adjacent channel grid points. Like *Kasemir* [1960], *Mansell et al.* [2002] assumed the overall neutrality of the channel, which was ensured by favoring the development of a part of the bidirectional tree having a charge deficit. In particular, if the overall net charge carried by the discharge trees after an iteration was positive (respectively negative), the threshold field needed for advancement of branches of negative (respectively positive) polarity was lowered to enhance their development until neutrality was achieved [*Mansell et al.*, 2002].

[9] The aforementioned channel-based simulations of lightning only model the leader part of the discharge. Nonetheless, it is well known that a streamer zone, not described in the previous models, develops at the leader tip and plays an important role in leader advancement [e.g., *Bazelyan and Raizer*, 2000, p. 71]. Because of its high conductivity, the leader is analogous to an equipotential metallic wire which gets polarized when placed in the thundercloud ambient electric field. The resulting accumulation of charge at the tip of the leader enhances the surrounding electric field above the threshold required for initiation of streamers. Consequently streamers continuously develop in the region surrounding the tip with a generation frequency on the order of 10^9 s^{-1} [*Bazelyan and Raizer*, 2000, p. 71]. The charge density associated with streamers leads to a self-consistent reduction of the electric field in the leader streamer zone to values comparable to the streamer initiation threshold [*Bazelyan and Raizer*, 2000, pp. 56–71]. In addition, currents of all streamers starting from a leader tip are summed up, heating the region ahead of the tip and therefore increasing its conductivity permitting further propagation of the leader channel [*Bazelyan and Raizer*, 2000, pp. 53–64 and 255; *Rakov and Uman*, 2003, pp. 136 and 226]. The exclusion of the direct modeling of the streamer zone in existing models is justified by the lack of knowledge of the detailed physics of this region as well as by the computational expenses involved in a thorough description of it.

[10] *Kupershtokh et al.* [2001] proposed to introduce the streamer zone in probabilistic lightning models using a cellular automata approach. *Kupershtokh et al.*'s [2001] model does not deal with the underlying physics of the process. Thus, from this point of view it remains close to *Niemeyer et al.*'s [1984] original model. The previous models consider only two states for any grid point in the domain: a conducting state, if the point is crossed by the leader, and a dielectric state otherwise. The use of a cellular automata approach described by *Kupershtokh et al.* [2001] allows the introduction of a third, streamer state, reproducing the streamer zone. Moreover, *Kupershtokh et al.* [2001] introduced time in their model to overcome the absence of an actual timescale in the *Niemeyer et al.* [1984]-based models. The model developed in by *Kupershtokh et al.* [2001] has not yet been applied to the modeling of leader development in realistic thundercloud configurations.

[11] *Agoris et al.* [2004] also introduced leader-streamer zone effects but still based their model on the "classical" *Niemeyer et al.*'s [1984] dielectric breakdown model. In addition, they used a timescale for propagation of streamer and leader bounds. The formation time of each streamer segment likely to propagate the discharge is derived using the assumption of a Weibull probability distribution function and compared to the time step of the current iteration (defined as the average of the times of formation of all candidate streamer bounds). Hence at each step, if the time of formation of a candidate streamer link is smaller than the time step of the current iteration, the link is added to the existing tree. Unlike the leader streamer corona mechanism described above, the formation of leader channels is considered to be done at constant velocity compared to streamer propagation (and therefore with a constant time step). Its driving mechanisms are the same as in the work by *Femia et al.* [1993], except that candidate leader bounds are now defined between the leader channels and points occupied by a streamer link. This model is run in a 2-D Cartesian simulation domain and no charge considerations are accounted for at any stage of the development of either streamer or leader channels. This model has been applied to the study of Franklin rod height impact on the striking distance and produced results in good agreement with experiments.

[12] In *Kupershtokh et al.*'s [2001] model as well as in any other model based on approaches proposed by *Niemeyer et al.* [1984], the channel propagates through grid points of a discretized 2-D or 3-D simulation domain. Therefore the channel propagation often takes unrealistically sharp angles. This issue has been addressed by *Helsdon and Poeppel* [2005]. These authors proposed to avoid grid dependency in a 3-D geometry by deriving the direction of the lightning propagation based on the location of random free electrons near the leader tip, and no longer in terms of the probability introduced by *Niemeyer et al.* [1984]. Stochasticity in this model is therefore introduced by the location of the free electrons, which is derived using a Monte Carlo technique [*Helsdon and Poeppel*, 2005]. The channel is assumed to be equipotential and the linear charge density is derived using the theory for unbranched conductors [e.g., *Mazur and Ruhnke*, 1998]. *Helsdon and Poeppel* [2005] have been able to identify numerical parameters of the model leading to the realistic behavior of the channel (e.g., branching, arresting of propagation, etc.), and the model produced positive leaders developing in the negative charge regions, and negative leaders propagating in the positive charge center, generally consistent with observations.

[13] The purpose of this paper is to present a new fractal model of lightning derived from *Niemeyer et al.*'s [1984] Dielectric Breakdown Model. The model is three-dimensional and uses *Kasemir*'s [1960] equipotential hypotheses to describe the channel properties. Special emphasis is placed on obtaining self-consistent solutions preserving complete charge neutrality of discharge trees at any stage of the simulation. This model is applied to investigation of changes in configuration of the thunderstorm electric field by an intracloud lightning discharge. The model results are directly compared to an intracloud discharge detected by the LMA.

[14] The study of cloud-to-ground discharges involves modeling of additional processes (e.g., the development of the return stroke) which requires further discussion and validation. The initial work on related subject has recently been presented by *Riousset et al.* [2006] and will be

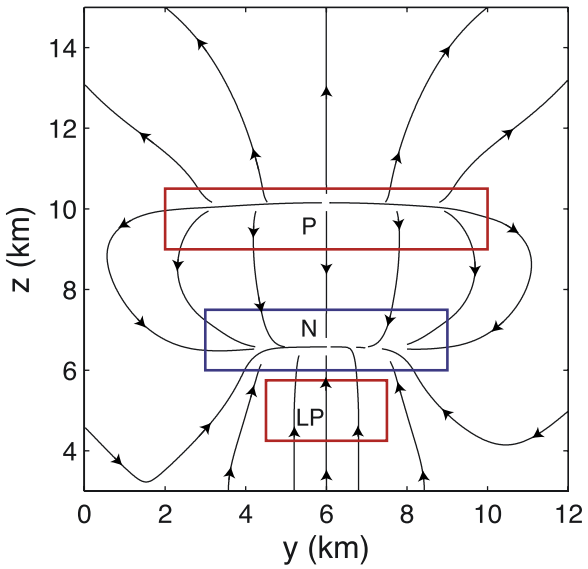

Figure 1. A cross-sectional view in the y–z plane at x = 6 km of the model thundercloud with upper positive (P), central negative (N) and lower positive (LP) charge layers. Electric field lines produced by the model cloud are also shown for reference.

reported in a separate paper. The present paper focuses on intracloud discharges only.

2. Model Formulation

[15] The thundercloud and lightning discharge are modeled in a 3-D Cartesian domain. The domain is discretized using equidistant grids (specific parameters are given in section 3).

[16] The thundercloud charge distribution is based on a tripole model [e.g., *Williams*, 1989; *Rakov and Uman*, 2003, p. 69]. This model is often regarded as an adequate approximation of the charge structure involved in lightning discharges in the convective parts of normally electrified storms. It employs a three layer charge structure above a perfectly electrically conducting (PEC) flat ground plane. A main negative charge (Q_N) is located at midlevels in the storm, with comparable upper positive charge (Q_P) above the negative and a weaker lower positive charge (Q_{LP}) below the negative, as illustrated in Figure 1. The model can also be extended to include negative screening charge (Q_{screen}) at the top of the cloud, but this extension is not implemented in the present study. An important aspect of storm charge structure is that the upper positive and main negative charge regions are spread in horizontally extended regions within the confines of the storm as will be further described below.

[17] The particular charge configuration used in our modeling closely follows the approach of *Krehbiel et al.* [2004] and *Behnke et al.* [2005]. Each charge layer is assumed to have a cylindrically symmetric disk shape with dimensions chosen on the basis of observations of a storm over Langmuir Laboratory on 31 July 1999, as determined by *Krehbiel et al.* [2004] and summarized in Table 1 (see *Marshall et al.* [2005] for results concerning the initiation conditions of cloud-to-ground lightning discharges in this storm). In the study by *Krehbiel et al.* [2004], charging currents I_1 and I_2 were introduced between the upper and lower dipolar structures (i.e., Q_N–Q_P and Q_N–Q_{LP}, respectively) that reproduced the average lightning rates of both cloud-to-ground and intracloud flashes, as determined by the three-dimensional Lightning Mapping Array (LMA). The charging currents were I_1 = +1.5 A between the main negative and upper positive, and I_2 = −90 mA between the main negative and lower positive charge regions. The resulting variation of the electric field profiles with space and time along the axis of the modeled charge structure reproduced the basic features of balloon-borne electric field soundings through the storm [*Krehbiel et al.*, 2004].

[18] In the present study, the above charging currents were applied until the conditions for initiation of an intracloud discharge between the main negative and upper positive charge regions were satisfied (discussed later in this paper). The charge brought by the currents was uniformly distributed in cylindrical disk volumes with dimensions specified in Table 1 (see also Figure 1). The values of the thundercloud charges at the time of the lightning initiation are also included in Table 1 for reference. The charge density of the model thunderstorm at the time of discharge initiation is discretized on the grid points of the simulation domain and referred to as the ambient charge density ρ_{amb}. From the charge density, the ambient electric field and potential ($\vec{E}_{amb}$ and ϕ_{amb}) are determined at all grid points within and on the boundaries of the simulation domain.

[19] The potential on the side and upper boundaries is calculated so that the contributions of all the charges within the simulation domain as well as the ground images of these charges are accounted for. Those boundary conditions are further referred to as "open boundaries." The ground is assumed to be a perfect conductor with potential $\phi_{gnd} = 0$. Consequently, the electric potential at the boundaries prior to the discharge can be obtained directly from the following expression [e.g., *Liu and Pasko*, 2006]:

$$\phi(\vec{r}) = \phi_{amb}(\vec{r}) = \frac{1}{4\pi\epsilon_0}\iiint_{V'}\frac{\rho_{amb}\left(\vec{r'}\right)}{|\vec{r}-\vec{r'}|}dV' + \frac{1}{4\pi\epsilon_0}\iiint_{V'}\frac{\rho^i_{amb}\left(\vec{r'_i}\right)}{|\vec{r}-\vec{r'_i}|}dV' \quad (1)$$

where $\vec{r}$ defines the coordinate vector of a point at a boundary and $\phi(\vec{r})$ the total potential at this point. The quantity $\rho_{amb}(\vec{r'})$ refers to the ambient charge density at point $\vec{r'}$, while $\rho^i_{amb}(\vec{r'_i})$ designates the ground image of the ambient charge distribution at point $\vec{r'_i}$. Having calculated potential values on the boundaries, we numerically solve

Table 1. Charge Values, Heights, and Extents for the Cylindrical Disk Model

Charge Layer	Altitude, km AGL[a]	Depth, km	Radius, km	Charge, C
P	6.75	1.5	4.0	48.7
N	3.75	1.5	3.0	−51.6
LP	2.00	1.5	1.5	2.92

[a]AGL, above ground level.

Poisson's equation $\nabla^2\phi_{amb} = -\rho_{amb}/\varepsilon_0$ using a SOR algorithm [e.g., *Hockney and Eastwood*, 1981, p. 179] to calculate ϕ_{amb} and $\vec{E}_{amb} = -\vec{\nabla}\phi_{amb}$ inside of the simulation domain. The development of discharge trees starts when the cloud charges reach values such that the ambient field exceeds a predefined initiation threshold E_{init} for a lightning discharge by 10% somewhere in the simulation domain (the related charge values are shown in Table 1). From this moment on, the ambient charge distribution remains unchanged.

[20] The exact value of the initiation threshold (i.e., of the electric field E_{init} required to initiate the lightning) is not well established, neither are the mechanisms of the lightning initiation [e.g., *Marshall et al.*, 1995; *Dwyer*, 2003; *Behnke et al.*, 2005, and references therein]. A general consensus exists in the present literature that values around $\sim$1–2 kV/cm at sea level represent a reasonable estimate of fields needed for lightning initiation [e.g., *Gurevich and Zybin*, 2001; *MacGorman et al.*, 2001; *Behnke et al.*, 2005; *Helsdon and Poeppel*, 2005; *Mansell et al.*, 2005; *Marshall et al.*, 2005]. For the purposes of this paper, we adopt a value E_{init} = 2.16 kV/cm similar to that used in recent studies of *Krehbiel et al.* [2004] and *Marshall et al.* [2005].

[21] We note that the field value $\simeq$2.16 kV/cm at sea level is the minimum field needed to balance the dynamic friction force in air on a relativistic electron with $\sim$1 MeV energy [e.g., *McCarthy and Parks*, 1992; *Gurevich et al.*, 1992; *Roussel-Dupré et al.*, 1994; *Lehtinen et al.*, 1999; *Gurevich and Zybin*, 2001]. However, we emphasize that similarly to our previous work [e.g., *Pasko and George*, 2002] we use 2.16 kV/cm only as a reference field, making no direct association of the relativistic runaway phenomenon and lightning initiation in our model. The intracloud discharge develops as a bidirectional leader from the inception point. Although controlled by different processes, the propagation of the positive or negative branches is known to require nearly identical electric fields [e.g., *Raizer*, 1991, p. 375; *Bazelyan and Raizer*, 1998, p. 253; *Rakov and Uman*, 2003, p. 322]. This propagation threshold, denoted $E_{th}^{\pm}$, is about 1 kV/cm in large laboratory gaps (several tens of meters long) [*Raizer*, 1991, p. 362] and can be substantially lower in case of lightning leaders [*Gallimberti et al.*, 2002, and references therein]. Both the lightning initiation E_{init} and propagation $E_{th}^{\pm}$ thresholds represent input parameters in our model. In the framework of the present paper, the increases or decreases in these thresholds would lead to corresponding increases or decreases in thundercloud charge values and densities and would not affect any principal conclusions derived from the present study. In this paper we simply assume the same initiation and propagation thresholds $E_{init} = E_{th}^{\pm} = \pm 2.16$ kV/cm, where E_{th}^{+} is positive and represents the propagation threshold of positive leaders, while E_{th}^{-} is negative and represents the propagation threshold of negative leaders. These values are given at sea level, and it is assumed that they vary proportionally to the neutral atmospheric density N at other altitudes. Practical considerations have led us to define every altitude z in our model with respect to the ground level (i.e., $z = 0$ is always referred to as ground level). However, sea level is the usual reference for neutral atmospheric density N. Since ground level and sea level do not always coincide (e.g., when considering measurements in New Mexico thunderstorms), it is judicious to introduce explicitly the difference between ground level and sea level and to denote it as z_{gnd}. Therefore, the initiation and propagation thresholds can be derived at any altitude z above ground using the following representation:

$$E_{init}(z) = E_{th}^{\pm}(z) = \pm 2.16\,\frac{N(z + z_{gnd})}{N_0}\ [\mathrm{kV/cm}] \qquad (2)$$

where N_0 is the value of the neutral density at sea level.

[22] As already noted above, the model thundercloud achieves a maturity state sufficient for lightning initiation when the corresponding ambient electric field exceeds the initiation threshold field by 10% somewhere in the simulation domain. As a result of this process, a region of high electric field exceeding the initiation threshold by 0 to 10% is created around the central vertical axis of the simulation domain between the upper positive and central negative charge layers. The inception point is chosen randomly in this region with no weighting on the basis of the ambient electric field magnitude. Thus every point at which $|E_{amb}| \geq |E_{init}|$ has equal probability to initiate the discharge. The leader channel propagates iteratively from this starting point; at each step, one and only one link is added (at either the upper or the lower end of the tree) and the potential is updated to ensure the overall neutrality of the channel. To illustrate the procedure, we start from an existing channel and describe each step required to achieve the next stage of the development of the discharge tree.

[23] We first define the total potential ϕ, which can be viewed as the ambient potential due to thundercloud charges modified by the presence of the lightning trees up to the current stage of development. Further propagation of the channel requires the knowledge of ϕ inside of the domain. How ϕ is determined will be discussed later in this section. At this point, we assume that the total potential has already been established and show how the next segment of the discharge tree is added. By the choice of the new link, we introduce stochasticity in the model. Starting from the existing channel, a new link is chosen among the candidates, which are defined as the possible links between the channel points and the neighboring points where the local electric field exceeds $E_{th}^{\pm}$. For each candidate link i, the local electric field E_i is calculated as $E_i = (\phi^{start} - \phi^{end})/l$, where ϕ^{start} and ϕ^{end} are the total potentials at the tips of the candidate link, and l is the length of the link. Consequently, a positive or negative leader will be able to propagate through a candidate link i if $E_i \geq E_{th}^{+}$ or $E_i \leq E_{th}^{-}$, respectively. Examples of candidates originating from two representative points on an existing discharge tree are shown in Figure 2a. The existing tree is represented using solid lines, while the candidate links are represented by dashed lines. Figure 2a is plotted in 2-D for the sake of clarity, and an extension to the 3-D geometry actually used by the model is straightforward. The probability of the channel growth associated with candidate link i is assigned as follows [e.g., *Wiesmann and Zeller*, 1986; *Femia et al.*, 1993]:

$$p_i = \frac{|E_i - E_{th}^{\pm}|^{\eta}}{\sum_i |E_i - E_{th}^{\pm}|^{\eta}} \qquad (3)$$

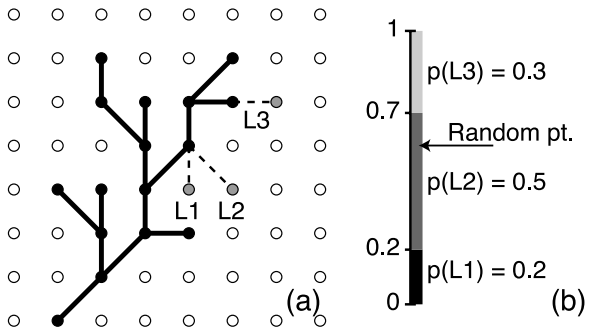

Figure 2. Channel extension in a 2-D geometry. (a) Channel links (solid lines) and link candidates (dashed lines) and (b) probability associated with each link. (The values of the probabilities given on this plot are arbitrary and are shown only for two representative points on the existing discharge tree for the purposes of illustration. Real values are derived on the basis of the analysis of potential differences involving all grid points of the existing discharge tree; see text for details.)

where η is called the probability sensitivity. The value of η has been derived by *Popov* [2002] to be 1 for streamer discharges in air. No similar derivation exists for the case of leader discharges. For all calculations presented in this paper, we adopt $\eta = 1$, which is a common choice in existing fractal models [e.g., *Niemeyer and Wiesmann*, 1987; *Mansell et al.*, 2002]. The probability associated with each link can be represented as a portion of a segment of unity length (see Figure 2b). By picking randomly a point between 0 and 1 on this segment, we select the new link. Therefore, this procedure accounts for both the propensity of the channel to develop in regions of strong electric field and for the stochastic nature of the leader development.

[24] Once the new link has been selected, the potential needs to be redefined in the channel, inside of the domain and at its boundaries. This potential adjustment, which has formerly been used for simple deterministic models [e.g., *Mazur and Ruhnke*, 1998], is the salient component of the model compared to the previous fractal modeling of lightning discharge [e.g., *Mansell et al.*, 2002], and must account for the overall neutrality of the discharge tree and its equipotentiality. This is achieved in the following way. From the principle of superposition, the total potential in the presence of a conducting tree at each point M inside the simulation domain can be written as $\phi(M) = \phi_{amb}(M) + \phi_{cha}(M)$, where $\phi_{cha}(M)$ is the potential due to the charges induced on the channel. In particular, for points P on the channel, $\phi_{cha}(P) = \phi_0 - \phi_{amb}(P)$ to make the channel an equipotential characterized by the constant potential ϕ_0. A simple iterative procedure is used to determine the value of channel potential ϕ_0 that minimizes the net charge on the channel as described later in this section. The updated values of ϕ_{cha} after the addition of a new link are derived by solving Laplace's equation $\nabla^2\phi_{cha} = 0$ using the SOR algorithm with Dirichlet's conditions (i.e., fixed potential) on the interior and exterior boundaries defined hereafter. The grid points occupied by the channel serve as an interior boundary, and the potential $\phi_{cha}(P)$ at these point is fixed and set to $\phi_0 - \phi_{amb}(P)$ as detailed previously. The values of the potential on the boundaries of the simulation domain define the exterior boundary. They are taken from potential solutions obtained after the previous link was added and are also assumed fixed. Having applied Poisson's equation to the new result for ϕ_{cha}, but now including the points on the channel in calculation of the Laplacian, we can estimate the charge density ρ_{cha} associated with the channel as $\rho_{cha} = -\varepsilon_0\nabla^2\phi_{cha}$. Since $\nabla^2\phi_{cha} = 0$ everywhere outside the grid points which belong to the discharge trees, ρ_{cha} is confined only to the grid points on the channel. The total charge Q_{cha} on the channel can then be obtained by performing an integration of ρ_{cha} over the volume of grid points associated with the discharge trees as follows: $Q_{cha} = \iiint_V \rho_{cha}(\vec{r})dV$. In addition, the electric dipole moment $\vec{p}$ of the discharge trees is derived for diagnostic purposes as: $\vec{p} = \iiint_V \vec{r}\rho_{cha}(\vec{r})dV$ [e.g., *Zahn*, 1987, p. 139].

[25] The value of ϕ_0 to achieve overall neutrality of the channel, namely $Q_{cha} = 0$, is determined by applying a bisection method [e.g., *Press et al.*, 1992, p. 353]. This root-finding algorithm requires that the solution is known to lie inside a given interval. For the present model, the total potential of the channel ϕ_0 will necessarily lie between the minimum and the maximum of the ambient potential. Because the algorithm quickly converges to the solution, we simply use the extrema of ϕ_{amb} to bound the solution instead of attempting to estimate ϕ_0 on the basis of its value at the previous stage of the channel development.

[26] Having determined ϕ_0 and ϕ_{cha} as described above, the effect of the channel is known everywhere in the simulation domain following addition of each new link. In particular, the determination of ρ_{cha} enables us to update the contribution of the channel to the potential at the simulation domain boundaries. This is done using equation (1) with ϕ_{amb}, ρ_{amb} and ρ^i_{amb} respectively replaced by ϕ_{cha}, ρ_{cha} and ρ^i_{cha}, where ρ^i_{cha} is the ground image of the channel charge. The recalculated values are used for the boundary conditions during the next step of the discharge development. Thus the update of the simulation domain boundary conditions is always "one link behind" with respect to advancement of the channel. This delay is due to the impossibility to determine the effect of a link on the boundary conditions prior to its establishment. Since the difference is only that due to the addition of a single link, the errors introduced by this approach are expected to be small. Typically, for the simulation results presented in the next section, a link modifies the total potential at the boundary by less than 1%. Even though the changes are small ($\leq$1%) during every step of the model execution, we fully recalculate the potential at the side and upper boundaries after each addition of a new link for maximum accuracy.

[27] Finally, recalling that ϕ_{amb} has been previously derived inside of the domain and at its boundaries, the potential at any point M of the domain can be obtained using the principle of superposition $\phi(M) = \phi_{cha}(M) + \phi_{amb}(M)$. At this stage, all requirements are fulfilled and model execution proceeds to development of the next link. This procedure is repeated until no candidate links for further extension can be found or until a point when a channel link reaches the ground. In the present paper, we focus on studies of intracloud discharges, which are more

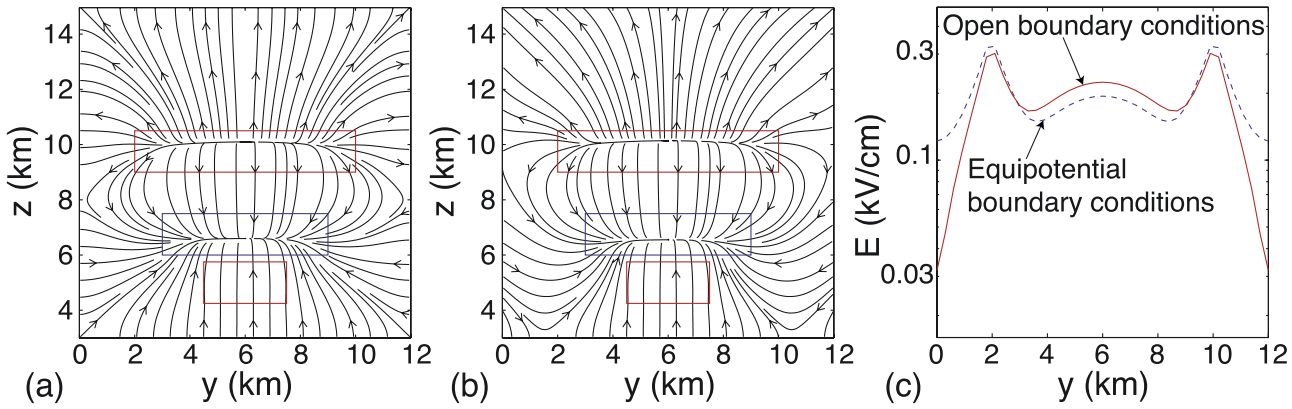

Figure 3. Electric field lines pattern of the thundercloud with parameters specified in Table 1 in a simulation domain with (a) equipotential boundaries and (b) open boundaries. (c) Comparison of the electric field magnitudes using equipotential (dashed line) and open boundary conditions (solid line) at an altitude of 9.8 km.

probable for thundercloud charge configuration specified at the beginning of this section.

3. Results

[28] In this section, we report results from a representative simulation run corresponding to an intracloud discharge. The results have been obtained in a 12 km × 12 km × 12 km simulation domain, which has been discretized using 41 × 41 × 61 equidistant grid points. Hence, the space resolution is 300 m in the x- and y-directions and 200 m in the vertical z-direction. We note that the ground level for lightning simulations is different from the reference altitude for the LMA measurements (which is usually within 10 m of the mean sea level [*Rison et al.*, 1999]). As discussed in the previous section, our model uses ground level as zero altitude ($z = 0$ km) reference point. To ease direct comparison with LMA results, all plot results produced by our model have been shifted by adding z_{gnd} to z such that all altitudes in Figures 1 and 3–8 are given with reference at the sea level. After ~32.5 s of application of charging currents I_1 and I_2 with magnitudes defined in the previous section, the conditions for lightning initiation are fulfilled (i.e., the electric field at one of the points inside of the simulation domain exceeds E_{init} threshold by 10%). This leads to cloud charge density ρ_{amb} in the two upper charge layers on the order of ±1 nC/m^3. These values are smaller than those inferred from measurements by *Williams et al.* [1985] or *Coleman et al.* [2003], but still of the same order of magnitude. The positions, dimensions and integral charge values corresponding to each charge layer at this moment of time are summarized in Table 1.

[29] Figure 1 shows a cross-sectional view of the model thundercloud (in the y–z plane positioned in the center of the simulation domain at x = 6 km). The upper and lower positive charge layers are identified by the letters P and LP respectively, while the central negative charge layer is identified by the letter N. In addition, Figure 1 also illustrates the electric field lines produced by this charge configuration just before the initiation of the discharge. The electric field lines converge toward the negative charge center and diverge from the upper positive one, consistent with expectations. At the lower boundary, the field is normal to the equipotential ground surface, also consistent with field theory.

[30] If equipotential boundaries with potential equal to ϕ_{gnd} were used, the field line pattern would be conspicuously modified close to the side and top boundaries, where the field lines would be normal to the edges of the domain. This modification is best seen if the number of field lines in Figure 1 is increased (Figure 3b), and the resulting field line pattern compared to that of the same thundercloud when equipotential boundaries are employed (Figure 3a). The magnitude of the electric field would also be modified by the use of equipotential boundary conditions. A comparison of the y-scan of the field magnitude at 9.8 km altitude (in the middle of the upper positive charge layer) and at the center of the simulation domain at x = 6 km (Figure 3c) shows that the use of equipotential boundary conditions introduces a noticeable error, in particular close to the boundaries. In particular, at y = 0 km, the field magnitude is ~3.2 × 10^3 V/m using the open boundary simulation domain, and ~1.2 × 10^4 V/m using equipotential boundaries. Hence equipotential boundaries are not suitable for narrow simulation domains such as the one employed in this study. We additionally note that in both cases the field magnitude is much greater than the fair weather field magnitude at the same altitude ~4.7 V/m [*Rakov and Uman*, 2003, p. 9].

[31] Figure 4 shows an example of a fully developed discharge. The discharges trees are projected on the x–z, x–y and y–z planes (shown, respectively in Figures 4b, 4d and 4e). Figure 4c shows a histogram representing the numbers of grid points occupied by the discharge links as a function of the altitude. Finally, the altitude of each new link at each step is plotted in Figure 4a. The sequence of steps in our model can be considered as resembling the temporal development of lightning flashes in the actual LMA measurements. The step number gives the sequence of creation of new links in the model, and a color scale similar to actual LMA data is used. For this run, ground level has been set at 3 km above sea level (the approximate altitude of the ground for measurements of the lightning activity near Langmuir Laboratory in central New Mexico).

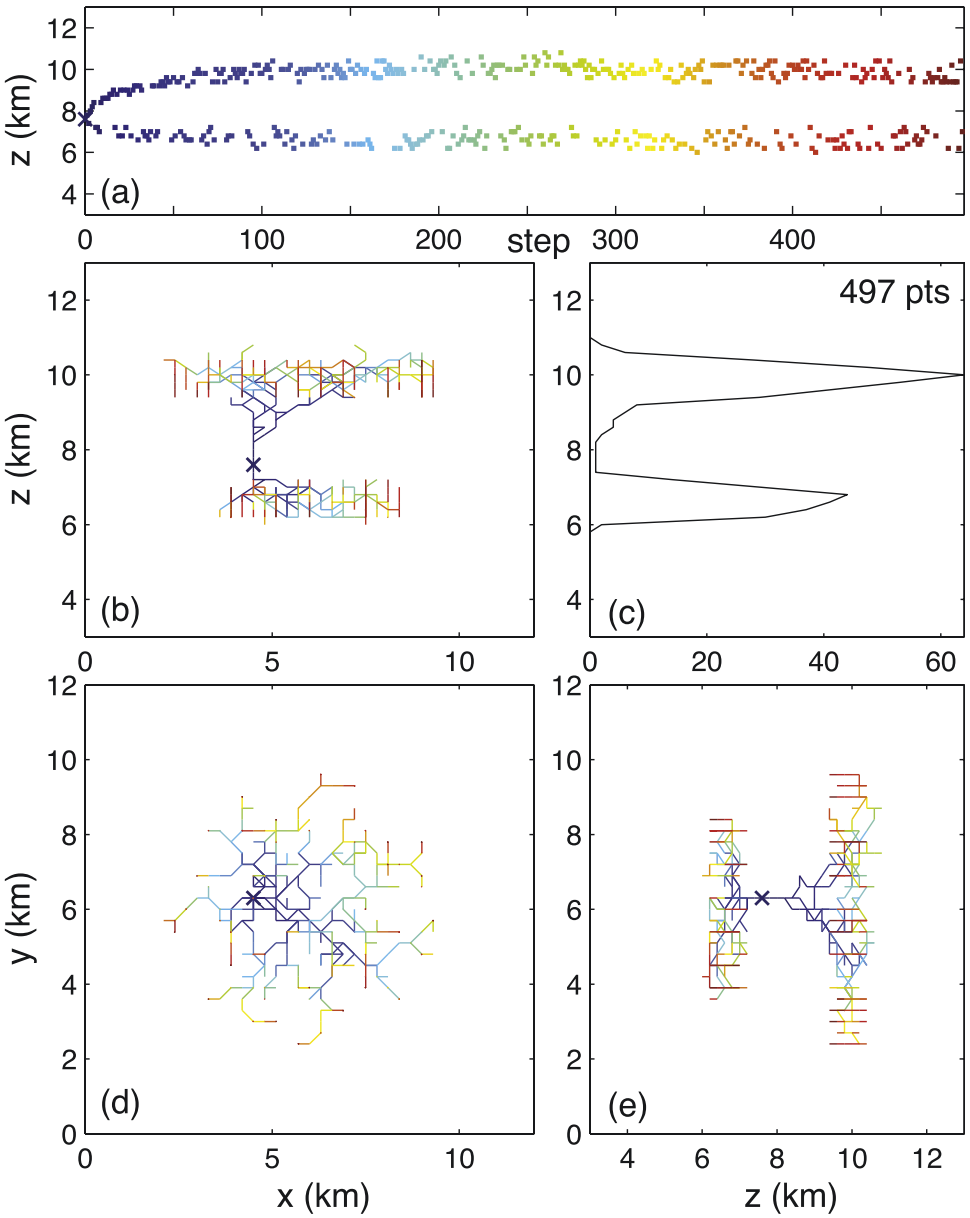

Figure 4. Representation in Lightning Mapping Array (LMA) data form of a simulated intracloud discharge. We use a formatting similar to that of the LMA data shown in Figure 5: (a) altitude of each new link, (b) a projection of the discharge links onto the x–z vertical plane, (c) altitude histogram representing the numbers of grid points occupied by the discharge links as a function of altitude, (d) a horizontal (plan) projection of the discharge links onto the x–y plane, and (e) a projection of the discharge links onto the y–z vertical plane. The crosses denote the position of the initiation of the discharge.

The topographic profile at the location of the LMA observations is presented by *Rison et al.* [1999] (Figures 3, 4 and 6) and justifies the assumption of a flat ground plane at the above altitude, due to the relatively small variations of the ground elevation ($\leq$1 km) in comparison with the altitudes of the charge centers and that of the development of the intracloud discharge (between 6 and 11 km, see Figure 5). The simulated discharge is initiated at an altitude of 7.6 km above sea level (4.6 km above ground level), $\sim$1.5 km radially away from the central vertical axis of the simulation domain. The developing leader initially extends vertically without showing much branching structure between $\sim$7.0 and $\sim$9.2 km before spreading horizontally in the volume of the main negative and upper positive charge layers (at altitudes around 6.5 and 10 km, respectively).

[32] Figure 5 presents an actual intracloud lightning detected by the LMA over Langmuir Laboratory on 31 July 1999 at 2223 (local time). This event is similar to the bilevel discharge first reported by *Rison et al.* [1999]. We note that the inception point of the discharge was at an altitude of $\sim$8.0 km on the southeastern edge of the storm. The discharge then propagates vertically between altitudes

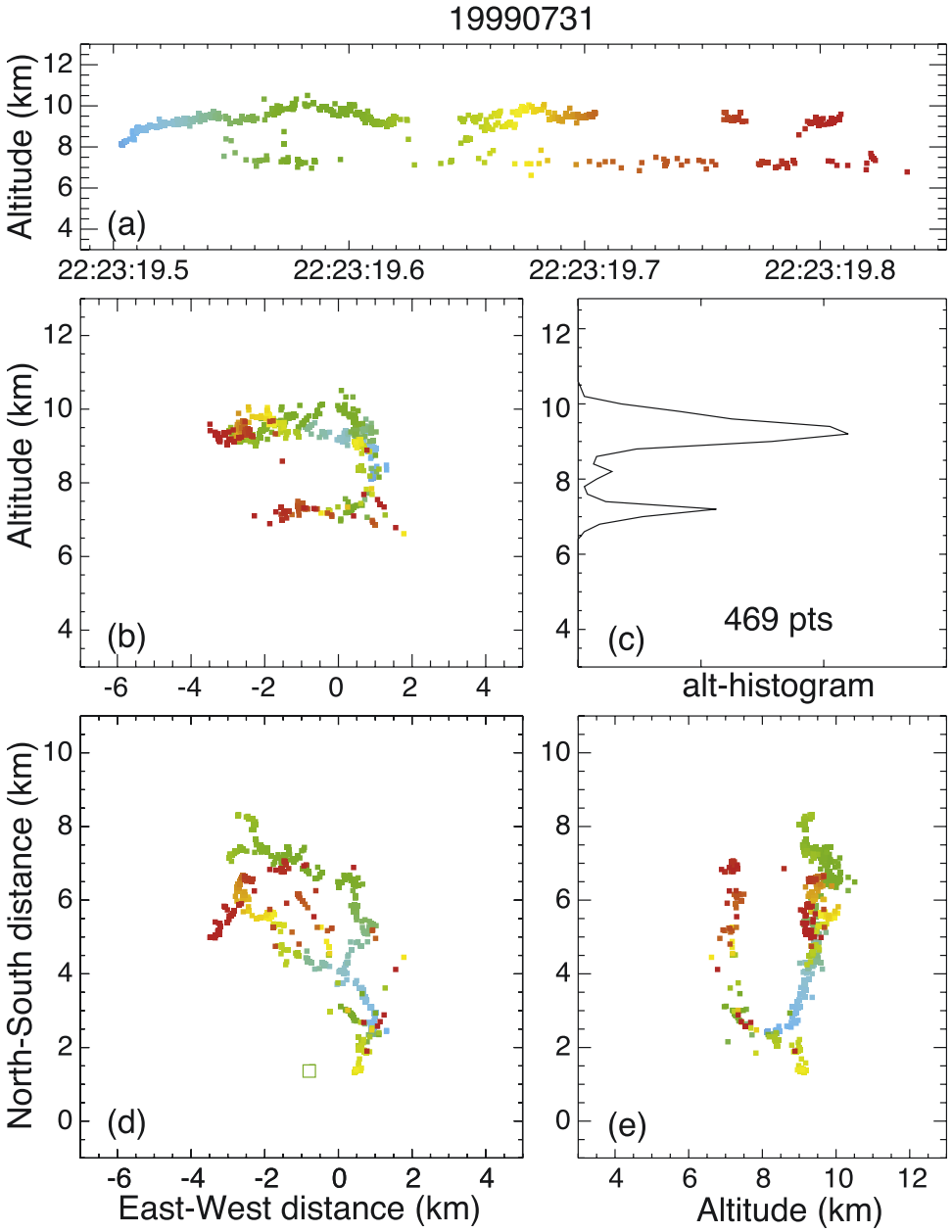

Figure 5. An actual bilevel intracloud flash measured by the LMA during the thunderstorm on 31 July 1999 at 2223 (local time). Locations of VHF radiation sources detected by the LMA are displayed using different formatting in five panels: (a) altitude versus time, (b) a projection of the sources onto the west–east vertical plane, (c) altitude histogram of the sources in 100-m bins, (d) a horizontal (plan) projection of the sources, and (e) a projection of the sources onto the south–north vertical plane.

around 7.0 and 9.0 km, where horizontal propagation then becomes dominant.

[33] Figure 6 is the same as Figure 4, except that only the branches developing above the initiation point are shown. In addition, we show the contours of the charge centers in Figures 6b, 6d and 6e by dashed gray lines. The upper positive, central negative and lower positive charge centers are shown in Figures 6b and 6e, while only the upper positive charge layer is illustrated in Figure 6d. Inspection of this figure shows that the negative leaders are essentially contained in the upper positive charge layer. Figure 7 is the same as Figure 4, except that now only the branches developing below the initiation point are shown. Similarly to Figure 6, we plotted the contours of the upper positive, central negative and lower positive charge centers in Figures 7b and 7e, and those of the central negative layer in Figure 7d. It can be noticed from this figure that positive leaders are mainly "trapped" in the central negative charge layer.

[34] Figure 8a shows the model discharge of Figure 4 in a 3-D representation, while Figures 8b and 8c compare respectively the total electric field and potential before and after the flash at the center of the simulation domain, along the vertical axis. The propagation threshold given by

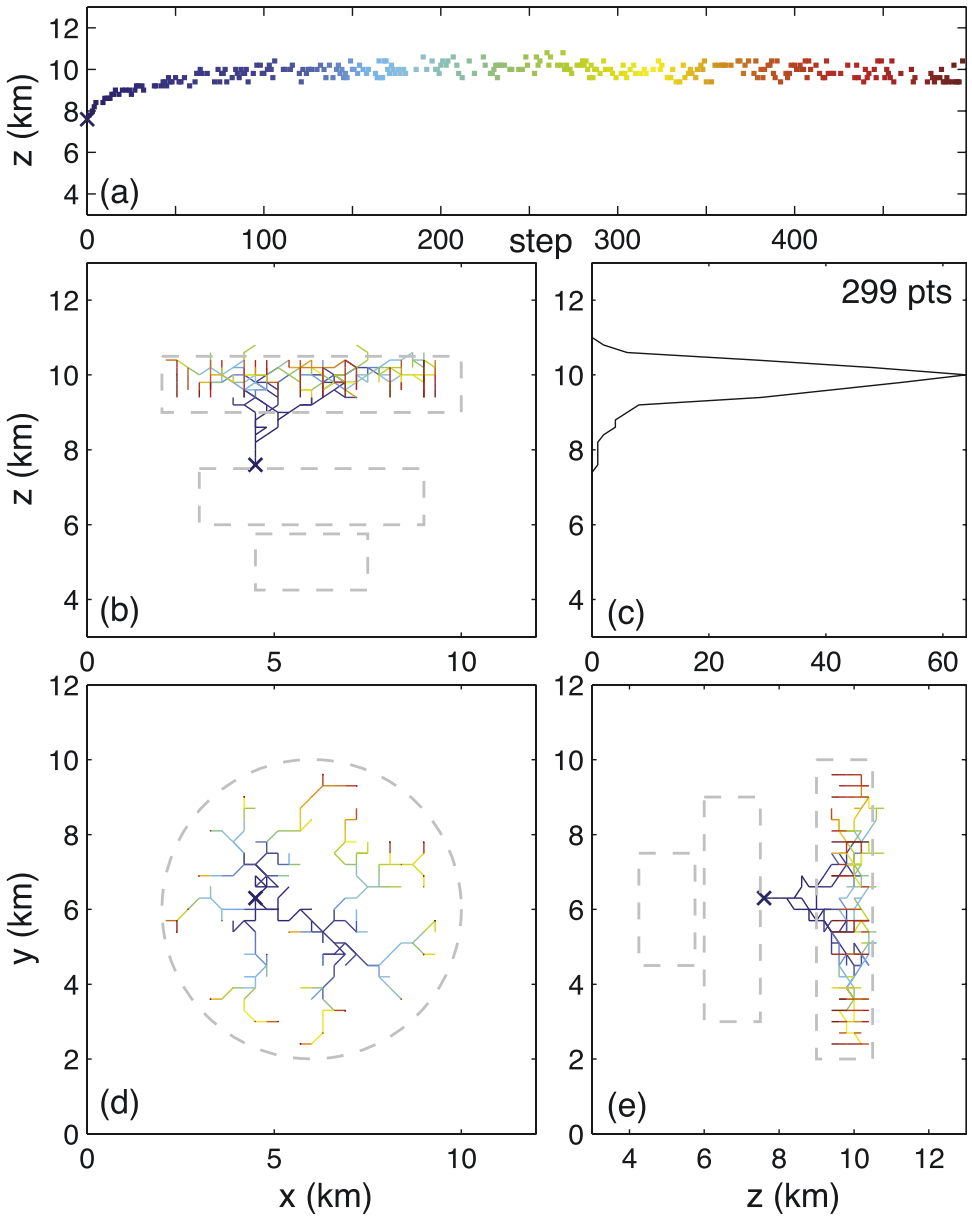

Figure 6. Representation in Lightning Mapping Array (LMA) data form of the upper branches of the simulated intracloud discharge reproduced in Figure 4. (a–e) Same as in Figure 4. The dashed gray lines represent the contours of the charge centers (see text for details).

equation (2) is also shown for reference in Figure 8b. A positive value of the electric field indicates an upward directed field.

[35] Figure 9a shows the evolution of the discharge tree total potential ϕ_0. The charge carried by the positive leaders is illustrated in Figure 9b. We note that negative leaders carry an equal amount of negative charge, and the charge shown in Figure 9b can be interpreted as the total charge transferred by the discharge. Figures 9c and 9d illustrate the evolution of the discharge dipole moment as the simulation progresses. Figure 9a shows a rapid increase of the channel potential at the early stages of the discharge development, from an initial value of −47.5 MV at the inception point, followed by a smoother increase after which ϕ_0 reaches the final value of ∼41.5 MV. Figure 9b shows a progressive growth of the charge transferred by the discharge which reaches value ∼37.5 C by the end of the simulation. The magnitude of the dipole moment $\vec{p}$ shown in Figure 9c also smoothly increases reaching ∼122 C·km. Figure 9c shows that $\vec{p}$ is predominantly vertical and directed downward. This trend is consistent with the development of the trees, since the horizontal components of $\vec{p}$ (i.e., p_x and p_y) become more and more negligible compared to the vertical component p_z.

[36] A comparison of the total charge in the system before and after the development of the discharge trees allows us to check the charge conservation. The system remains approximately neutral, with differences between absolute values of positive and negative charges not exceeding ∼30 mC during different stages of the model execution. This difference is mainly due to numerical noise and is negligible

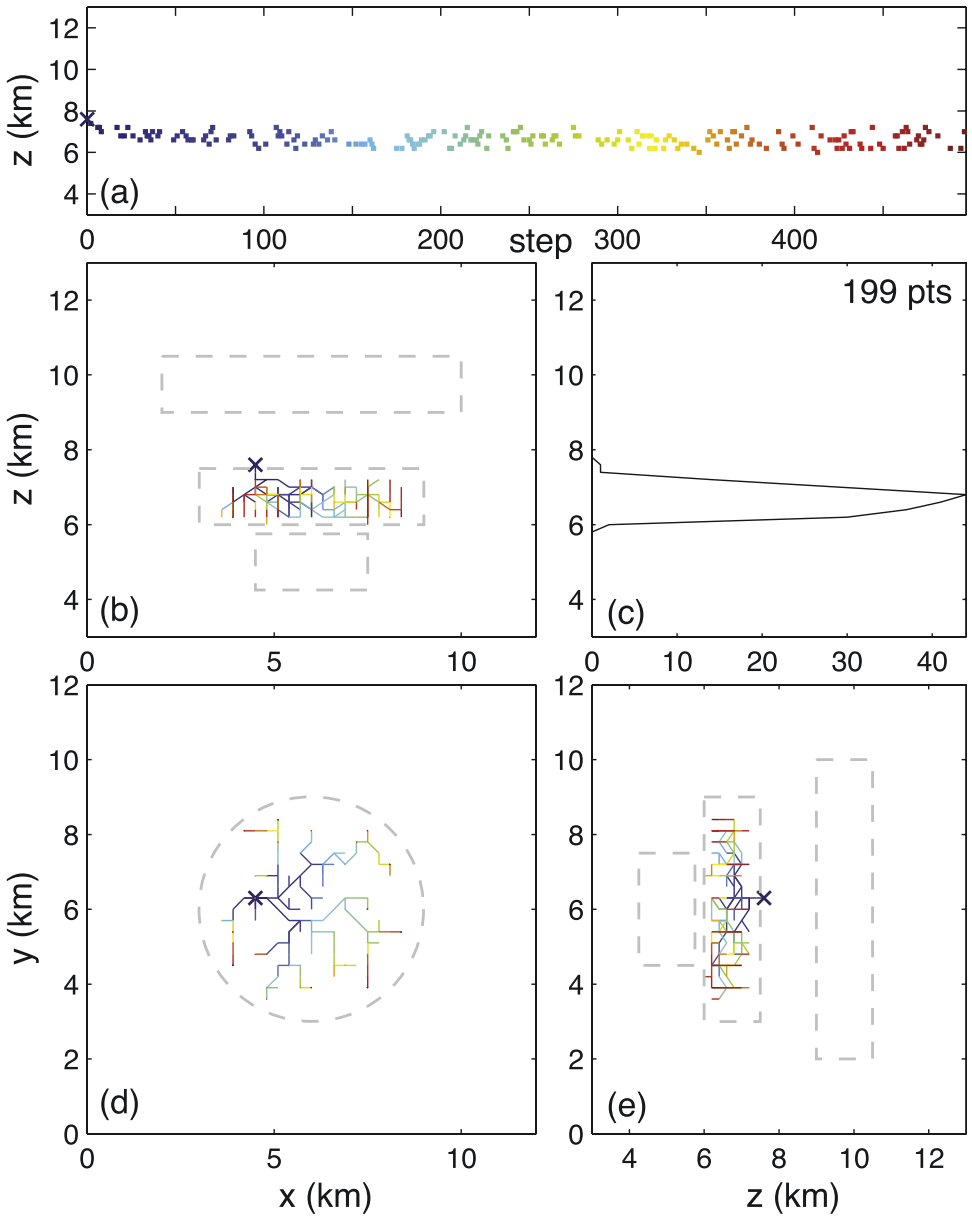

Figure 7. Representation in Lightning Mapping Array (LMA) data form of the lower branches of the simulated intracloud discharge reproduced in Figure 4. (a–e) Same as in Figure 4. The dashed gray lines represent the contours of the charge centers (see text for details).

compared to the charge in the cloud or in the upper and lower channel structures. As already noted above, the amount of charge carried by the positive and negative leaders is ~37.5 C, which constitutes ~75% of thundercloud charges of each polarity (i.e., 51.6 C) as shown in Table 1.

4. Discussion

[37] Advanced fractal modeling accounting for the charge neutrality of the discharge has been reported by *Mansell et al.* [2002]. Although both this model and ours make use of similar hypotheses (namely neutrality of the channel and equipotentiality or quasi-equipotentiality of the channel), the treatments of the channel neutrality and of the boundary conditions differ and constitute two salient improvements of our model.

[38] Unlike other fractal models referenced in section 1, our model modifies the channel potential as the discharge propagates. Previous models involving the charge neutrality of the channel have employed mathematical artifacts to ensure electric neutrality of the discharge, e.g., by varying the propagation thresholds [*Mansell et al.*, 2002]. In contrast to these models, we have chosen to develop a solution involving a physics-based potential variation. This solution avoids the introduction of additional parameters such as the percentage of charge imbalance allowed during the simulation run and the range of variation of the propagation thresholds. Furthermore, it ensures the neutrality at each stage of advancement of the discharge.

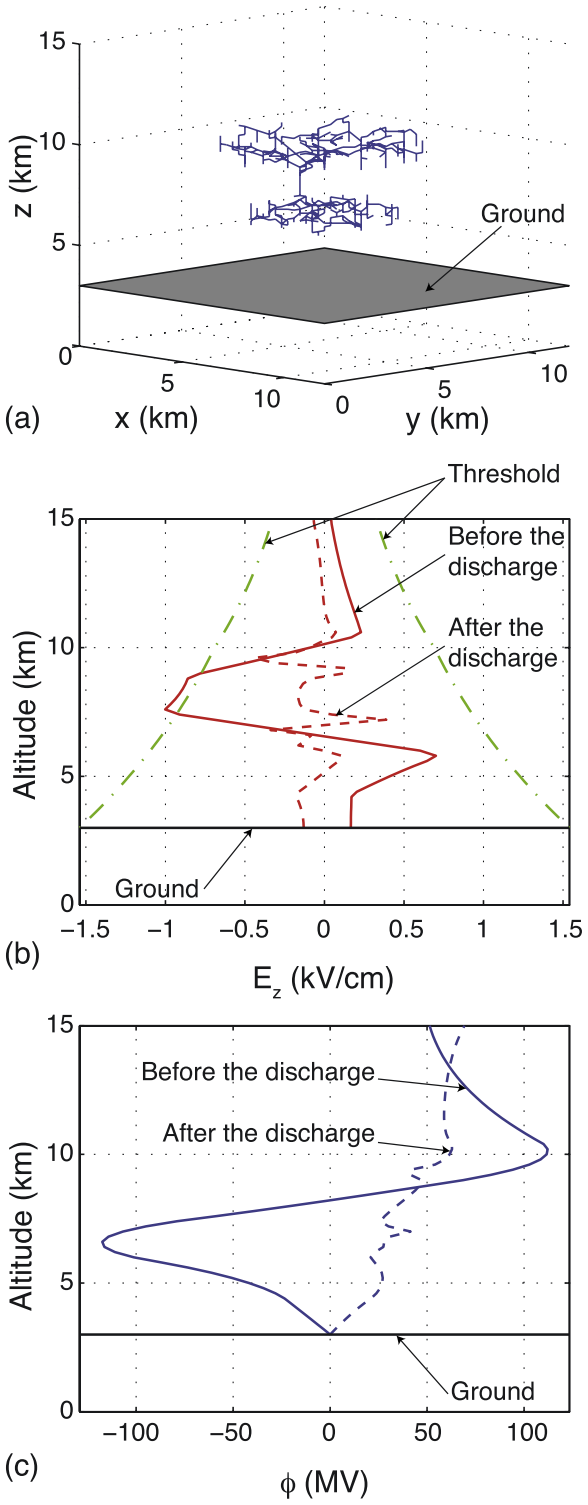

Figure 8. (a) Three-dimensional view of the intracloud discharge shown in Figure 4 after 496 steps. (b) Electric field before the flash (solid line) and after (dashed line) along the central vertical axis of the simulation domain. The electric field initiation threshold is shown for reference by dash-dotted lines. (c) Electric potential before (solid line) and after (dashed line) the discharge development along the same axis.

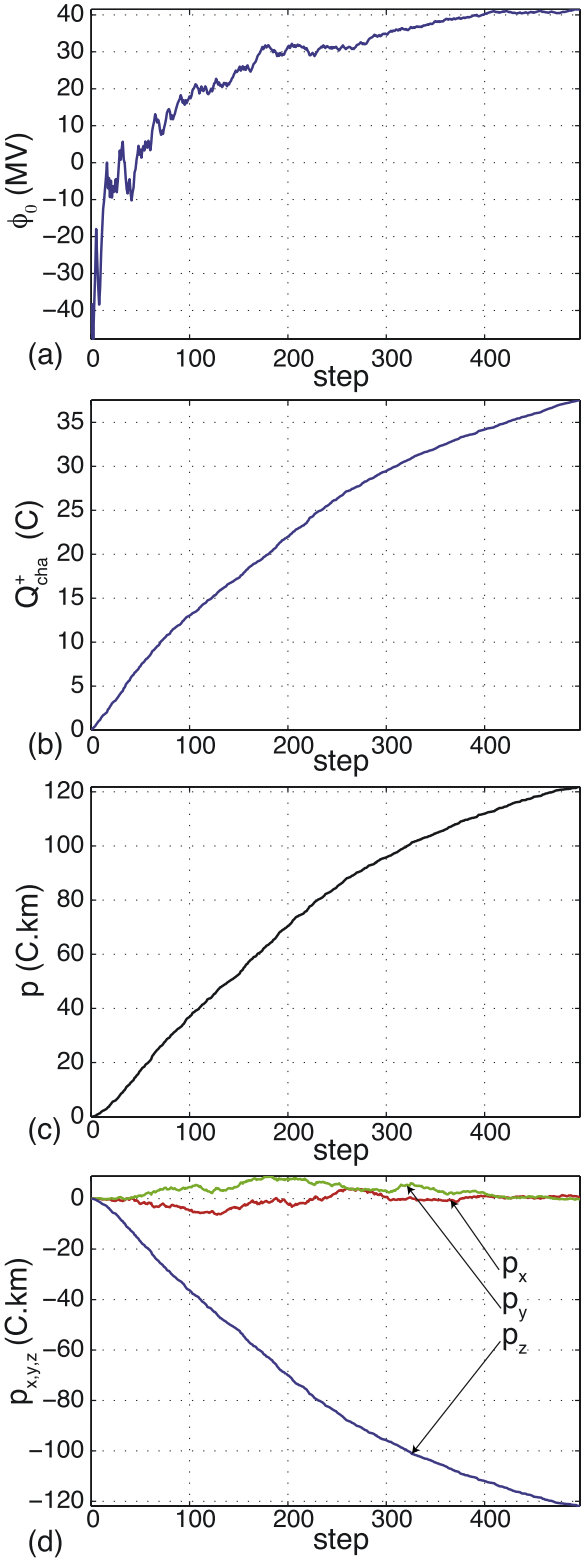

Figure 9. Parameters of the simulated discharge shown in Figure 4 at each step of the development: (a) channel potential ϕ_0; (b) charge carried by the positive leaders Q^+_{cha}; (c) magnitude of the discharge electric dipole moment $p = |\vec{p}|$; and (d) x-, y- and z-components of the dipole moment $\vec{p}$.

[39] The treatment of the boundary conditions also represents a significant improvement compared to previous lightning models. While simple, fixed Dirichlet's and/or Neumann's conditions have commonly been used in previous modeling [e.g., *Mansell et al.*, 2002], the choice of a similar Dirichlet's condition at the ground but open boundary conditions on the upper and side boundaries (see section 2) allows to simulate an open domain in order to obtain a better modeling of the mirror charges. Also, this solution lets us place the boundaries closer to the charge centers, hence yielding increased resolution in the simulation domain, which is of major importance for further advancement of lightning simulation studies.

[40] The simulation run described in section 3 is typical for intracloud discharges produced by our model. As will be discussed in this section, it shows many similarities with the bilevel discharge observed during the thunderstorm over Langmuir Laboratory on 31 July 1999, which is reproduced in Figure 5. Comparability between fractal modeling and lightning mapping data was mentioned by *Mansell et al.* [2002]. The present paper further develops the comparison between real and model lightning discharges and introduces a quantitative evaluation of the simulation results.

[41] The LMA observations (Figure 5) show the initial 2–3 km vertical propagation followed by two distinct regions of roughly horizontal propagation at altitudes of ~6.5 and ~9.5 km. The upper region corresponds to the propagation of the negative leaders in the thundercloud positive charge, and the lower one to that of the positive leaders in the main negative charge. The propagation altitudes of the model discharge are mostly defined by the chosen positions of the model thundercloud charges, which are inferred directly from observations of real lightning discharges following the conclusions by *Coleman et al.* [2003]. Consequently, the model discharge (Figure 4) develops in the two upper charge layers at altitudes matching the altitudes of propagation of the real discharge (Figure 5).

[42] Comparison of Figures 4 and 5 shows that both the simulated and measured discharges are not initiated on the axis of the inferred storm charges, although they both propagate in a rather symmetric manner toward and in the upper positive and central negative charge layers. It is recalled that the x- and y-directions in our simulation are arbitrary and do not necessarily correspond to east–west and north–south directions in Figure 5. Thus no conclusions should be drawn from the horizontal position of the initiation point, it should merely be noticed instead, that our initiation algorithm produced realistic horizontal displacement of the initiation point with respect to the axis of the storm charge layers. The random initiation algorithm employed in the simulation uses the idea that the lightning is probably not initiated immediately upon the threshold being exceeded at some point in the cloud, but after the threshold is overexceeded over some larger horizontal area. Initiating the discharge once the threshold is exceeded by 10% somewhere in the simulation domain allows the growing charges Q_{LP}, Q_N and Q_P to create such a region around the central vertical axis. The lightning is then initiated randomly within this area of high electric field (exceeding the initiation threshold E_{init}).

[43] The initiation point should be regarded primarily as an indicator for locations of strongest vertical fields. In realistic situations the initiation point is also expected to depend on the nonuniformity of the actual storm charges. It is very improbable that the real thundercloud has the perfect cylindrical symmetry assumed by the model. Therefore a nonuniform charge distribution is considered as a primary factor which would lead to the lightning being initiated away from the center of the charge region as in the case of Figure 5.

[44] Tests have also been conducted with nonrandom initiation (the related results are not shown in this paper for the sake of brevity). In this case, the discharge was always initiated at the point of maximum electric field magnitude. Because of the cylindrical geometry of the modeled thundercloud, this point was always on the main axis of the inferred charge layers at an altitude of 7.6 km. The same initial 2–3 km vertical extension of the tree followed by the horizontal propagations at altitudes around 6.5 and 10.0 km was observed. The main difference was that the discharge had taken a more symmetric form since the horizontal shift of the initiation point was suppressed. Quantitatively, the values for the channel potential, transferred charge, linear charge density and dipole moments remained very close to those discussed for the simulation presented in Figures 4 and 8 with parameters shown in Figure 9.

[45] When the contours outlining the positions of the charge layers are superimposed with the discharge channels, as in Figures 6 and 7, it becomes obvious that simulated trees tend to propagate more or less through the full extent of the parent storm charges. A similar effect has been observed for dielectric breakdown in polymethylmethacrylate (PMMA) [*Williams et al.*, 1985]. This property has also been suggested for real intracloud discharges [e.g., *Shao and Krehbiel*, 1996; *Coleman et al.*, 2003] and has been noticed in previous fractal modeling of lightning [*Mansell et al.*, 2002]. However, the complexity of the charge structures involved in both observations and *Mansell et al.*'s [2002] simulation results makes it difficult to interpret the full extent of the effects of net charges on the development of the channel. In particular, while *Mansell et al.*'s [2002] results show that the leader channels penetrate regions of net charge, the use of a simpler thundercloud charge structure in our model demonstrates that the discharge tends to be strongly limited or confined to such charge regions. This approach is comparable to *Williams et al.*'s [1985] experiments in charged and uncharged polymethylmethacrylate to test the effects of net charge on propagation of discharge trees (see also *Mansell et al.*'s [2002] numerical modeling interpretation of these experiments). This phenomenon can be explained by considering the dramatic changes in the field configuration prior to the discharge (represented in Figure 1) caused by the development of the lightning leader tree. In the leader breakdown process, the electric field lines are along the potential gradient between the channel potential and the surrounding ambient potential [*Riousset*, 2006, Figures 2.9 and 2.11 and pp. 22–30]. Specifically, when a conducting leader channel approaches and progresses into a region of intense charge, the field lines will connect the negative (respectively positive) charges induced on the channel and the surrounding positive (respectively negative) charges of the charge regions. Because of the large horizontal extension of the charge

centers, the field lines become primarily horizontal and the field intensity is also increased in this direction. Since the discharge path is mainly driven by the direction of the local electrostatic field, both in real [*Williams et al.*, 1985] and simulated clouds, it is expected that the upper and lower ends of the discharge tree would propagate horizontally inside of the charge layers.

[46] A comparison of Figures 4a, 4b, 4c, 5a, 5b, and 5c reveals a far greater number of points for the propagation of the simulated positive leaders when compared to the actual measurements. *Rison et al.* [1999] noted that negative breakdown in positive charge regions is inherently noisier at radio frequencies than positive breakdown in a negative layer. The LMA primarily detects the negative breakdown in the positive charge region. In the negative charge regions VHF radiation is produced primarily by recoil-type breakdown in which negative leaders reionize the channels formed by positive leader breakdown [*Shao and Krehbiel*, 1996; *Shao et al.*, 1996]. It appears that the LMA is locating such recoil activity in the negative charge regions. Recoil processes are not accounted for in our model. The model thus simulates what the LMA detects because of negative leaders, but not positive leaders. Yet, comparison of Figures 6 and 7 reveals that positive trees developing in the lower portion of the discharge occupy less grid points than negative ones. This effect is purely numerical (i.e., is not related to physical differences between different types of leaders observed in LMA data). Indeed, the upper positive and central negative charge centers have different radii (4 and 3 km, respectively) but are discretized using grids with identical grid size. Thus to extend through the entire volume of each charge layer, the discharge should require $(\pi R_P^2 d_P)/(\pi R_N^2 d_N)$ times as many steps in the positive as in the negative charge region. Here, R_P, d_P designate, respectively, the radius and depth of the upper positive charge layer, while R_N, d_N refer to the same quantities for the central negative charge region. Using values tabulated in Table 1, we calculate this ratio to be $\sim$1.78, which is in good agreement with the ratio derived $\sim$1.51 from Figures 6c and 7c.

[47] Comparison of Figures 4d and 5d emphasizes a major difference in the horizontal development in the simulated discharges as compared to the measured ones, namely the horizontal structure of the simulated trees looks far more complex. As noted previously, LMA measurements appear primarily to detect negative polarity, recoil-type breakdown associated with positive leaders, therefore the LMA map of negative leaders closely matches the map of modeled negative channels (Figure 6) but the LMA map of positive leaders has a different and simpler pattern than that of the modeled positive channels (Figure 7). Additionally, inspection of Figures 6d and 7d shows little difference between horizontal developments of positive and negative trees. The present version of the model does not include any differences between positive and negative leaders, and their streamer zones in particular, and an extension of the model to account for related effects represents a subject of future studies. It is also most likely that the details and complexities of the storm charge structure, which are not reproduced in our model, are largely responsible for the observed discharge structure shown in Figure 5.

[48] The calculated value of the charge carried by the leader trees has been estimated at every step of the simulation and is plotted for positive branches in Figure 9b. The value at the end of the discharge development, $\sim$37.5 C is of particular interest and can be compared to the values obtained from both observational and modeling studies. From multistation electric field change measurements, *Krehbiel* [1981] determined that the charge transfer during the first twelve intracloud discharges in a small developing Florida thunderstorm steadily increased from about 3 C for the initial intracloud discharge to 21 C for the twelfth discharge [see also *Krehbiel et al.*, 1984b]. In addition, the charge transfer for an energetic intracloud discharge in a fully developed storm was estimated to have been about 50 C [*Krehbiel et al.*, 1984a; *Shao and Krehbiel*, 1996]. *Helsdon et al.* [1992] quote typical values for the charge transferred ranging between 0.3 and 100 C. *Shao and Krehbiel* [1996] estimated charge transfer to be 8.5 and 49 C for two intracloud discharges in Florida on the basis of interferometer data and single-station electric field change measurements. *Rakov and Uman* [2003, p. 325] list the charge transfer values between 21 and 32 C for an intracloud discharge in a New Mexico thunderstorm. Previous fractal modeling of intracloud discharges estimated the charge transfer between 36.3 and 52.4 C [*Mansell et al.*, 2002, Figures 7 and 8]. Our model results are generally consistent with values documented in the existing literature.

[49] The average linear charge density of discharge trees in our model can also be estimated and compared to previously published values. This is done by summing the absolute value of the charge carried by channels of each polarity and dividing it by the total length of the channels ($\sim$147 km), leading to an estimate $\sim$0.5 mC/m. This value is below but still is in a reasonable agreement with a value of 1 mC/m referred to by *Helsdon et al.* [1992] and *Mazur and Ruhnke* [1998]. It is in also in good agreement with the linear charge densities between 0.7 and 8.7 mC/m estimated by *Proctor* [1997] for intracloud flashes with origin similar to that of the simulated discharge presented in this paper.

[50] Figure 9a shows the evolution of the channel potential during the development of the discharge trees. Being initiated just above the central negative layer, the initial channel potential ϕ_0 is strongly negative ($\simeq -47.5$ MV). In the early stages of the development ($\sim$30 steps), while the breakdown tree is developing vertically, ϕ_0 rapidly increases to approximately 0 MV. This change in potential is required to maintain channel neutrality in an asymmetric potential environment. In particular, the induced charge density along a linear, vertical equipotential channel is proportional to the difference between the channel potential and the ambient thundercloud potential at the same altitude. To maintain overall charge neutrality in the presence of an asymmetric potential profile, the leader potential changes as the breakdown increases in vertical extent [e.g., *Mazur and Ruhnke*, 1998; *Bazelyan and Raizer*, 2000, pp. 152–153; *Behnke et al.*, 2005, Figures 5 and 6]. For the simulation of this study, the negative and upper positive charges are nearly equal and opposite and the lower positive charge is relatively weak, so that the ambient potential profile becomes approximately symmetric when the channel potential ϕ_0 reaches about 0 MV (Figure 8c). Beyond $\sim$30 iteration steps, the channel has entered the upper positive charge region and starts

developing horizontally (Figure 4a). The channel potential continues to increase at a slower rate because of changes in the neutral midpoint location as the discharge develops, but more importantly because of substantial changes in the ambient potential profile and as the thundercloud becomes increasingly discharged. The channel potential at the end of the simulated discharge is about +41.5 MV, indicative of the potential of the discharged storm at the end of the discharge (Figure 8c).

[51] The regions of intense charge correspond to wells of ambient potential [*Coleman et al.*, 2003], i.e., extrema of the ambient potential bounded by strong potential gradients. For the simulation of this study, the potential wells are at altitudes of 6.6 km and 10.2 km (Figure 8c). Equation (3) emphasizes that the discharge develops into regions where the difference between the channel potential ϕ_0 and the surrounding potential (i.e., the ambient potential as modified by the presence of the channel) is maximized. The region where the discharge is initiated is a region of high potential gradients, therefore the discharge rapidly propagates ''downhill,'' that is to say in the direction of the strongest gradients, into and within the potential wells. The wells extend largely in horizontal directions (5–6 km) but are fairly narrow in the vertical direction (1–2 km). Thus, when the channel reaches the bottom of a well, further propagation in the z-direction would require it to go ''uphill,'' i.e., toward a decreased potential difference, while horizontal propagation allows the development of the discharge trees into the region where the difference between the channel potential and the surrounding potential is still large. In other words, the discharge starts developing horizontally because of greater potential gradients in the horizontal direction than in the vertical direction. Similar dynamics were observed by *Coleman et al.* [2003] for discharges detected by the LMA.

[52] It is noted that the altitudes of the potential extrema are slightly different than the altitudes of the charge centers (10.2 km versus 9.75 km for the upper positive charge, respectively, and 6.6 km versus 6.75 km for the negative charge). As noted by *Coleman et al.* [2003], the extrema in the vertical potential profile occur where the vertical component of the electric field E_z happens to pass through zero (Figure 8b). The zero crossings are influenced by the presence of multiple charge layers as well as by their locations, polarities and charge contents, causing the altitudes of the potential extrema to be different from those of the isolated charge centers. An important question is where the lightning-deposited charge will be centered. In terms of grid points involved in the simulated discharge, the number of grid points occupied by a discharge channel peaked at altitudes of 10.0 km and 6.8 km in the upper positive and midlevel negative regions, respectively (Figure 4c). These peaks were thus displaced somewhat from the altitudes of the potential wells, closer to or at the charge centers themselves. A more detailed understanding of the effects is the subject of continued study.

[53] The overall symmetry of the thunderstorm charge configuration in our model suggests that the resulting discharge electric dipole moment would be essentially vertical. The Q_P and Q_N charge layers form a normal polarity dipole in the upper part of the cloud in which leaders of opposite polarities propagate. It is therefore expected the fully developed channels would form an opposite polarity dipole (i.e., vertical and preferentially downward directed). Results presented in Figure 9d are consistent with these expectations. Figure 9d also indicates that the dipole moment of the discharge is dominated by its vertical component during the full period of propagation of the leader channels. The magnitude of the dipole moment of the fully developed discharge has been calculated to be ~122 C·km, as compared to the observational values reported by *Krehbiel* [1981] of 13–102 C·km for the initial intracloud discharges in a developing storm and ~200 C·km for the energetic intracloud discharge in a fully developed storm, and inferred dipole moment changes of 17 C·km and 147 C·km for the two intracloud discharges studied by *Shao and Krehbiel* [1996]. The results are also consistent with modeling results by *Mansell et al.* [2002], whose simulations estimated $|\vec{p}|$ = 173–241 C·km.

[54] The model also allows direct investigation of the reduction of the electric field inside of the thundercloud due to the growth of the discharge trees. The results shown in Figure 8b demonstrate that the simulated intracloud leader structure significantly reduces the electric field in the cloud. In particular, the fractional decrease of the electric field by ~80% at an altitude around 8 km is in reasonable agreement with the values ~60% and ~75% measured by *Winn and Byerley* [1975] and *Stolzenburg et al.* [2007], respectively. This reduction is especially pronounced at altitudes ~6.5 km and ~10.0 km, where most of discharge trees develop (see Figure 8b). The field is lowered far below the propagation threshold. Our results therefore demonstrate that under model conditions discussed in this paper the bulk charge carried by the integral action of positive and negative lightning leaders is sufficient to significantly reduce the value of the electric field in the thundercloud. Alternatively, these results also suggest that the location of the charge deposited by the lightning leader channels can be inferred from the location of strong field reduction in balloon sounding data.

[55] Results of the present study demonstrate the ability of the model to produce realistic intracloud discharges. In so doing, our results further support and expand upon the idea that lightning propagates through regions of net charge in a thunderstorm, and indicate the extent to which the two are coupled. The simulations also demonstrate that branching occurs primarily within the charge regions and, except for the leaders connecting the charge regions, the breakdown is effectively confined to these charge regions.

[56] A simple explanation for the propagation of lightning through regions of net charge rests on the assumption that discharges will tend to minimize the overall electrical energy of a storm, and that this will not be accomplished if the lightning deposited charges are displaced from the centers of the storm charges themselves (or from the potential wells). *Vonnegut* [1983] raised the question of the simplicity of the relationship between the lightning and storm charges for a phenomenon as complex as lightning. The issue has been partly resolved by the laboratory experiments of *Williams et al.* [1985] and by the recent observational studies by *Coleman et al.* [2003] and *Rust et al.* [2005]. These studies clearly established the existence of a close relationship between the lightning and storm charges and showed that lightning charge deposition partially

explains the complex charge structures observed by in situ measurements [*Rust and Marshall*, 1996; *Stolzenburg et al.*, 1998]. However, complete validation of the hypothesis requires simulation of the physics of the process as in the present study and the study by *Mansell et al.* [2002].

[57] The present study has tested the above ideas by (1) using lightning data to infer a realistic storm charge structure, (2) growing the charge structure to the point where it would be expected to produce lightning, (3) simulating the lightning with physical models, and (4) comparing the results. The fact that the results compare favorably shows not only that the modeling has been successfully implemented, but more importantly just how lightning responds to the storm charge distribution. Further studies and development of the model is expected to advance these ideas further yet. The results of Figure 8b demonstrate that the simulated intracloud leader structure reduces the overall electric field inside the thundercloud. At the same time, the field will be locally enhanced in the vicinity of the lightning channels, which can be investigated with further refinements of the model.

5. Conclusions

[58] In this paper a new model of intracloud lightning discharge has been presented, based on *Kasemir*'s [1960] hypotheses of equipotentiality and neutrality of the channel, and on the dielectric breakdown model proposed by *Niemeyer et al.* [1984]. Using a realistic thundercloud charge distribution, the model is able to reproduce a realistic pattern of an intracloud discharge (in particular, the altitude of initiation and extensive horizontal propagation of leader channels) comparable to an actual discharge observed over Langmuir Laboratory on 31 July 1999. It has been shown that parameters of the discharge such as the charge carried, dipole moment and average linear charge density associated with the leader trees, are in good agreement with previous modeling and related measurements reported in the existing refereed literature. The model has been applied to study the reduction of the electric field in the thunderstorm due to the growth of the bipolar structure of leader trees resembling development of an intracloud lightning discharge. This study suggests that the polarization charges carried by the leader trees could lower the net charge in the different charge layers of the thundercloud and could decrease the total electric field significantly below the lightning initiation threshold.

[59] **Acknowledgments.** This research was supported by the National Science Foundation under grant ATM-0134838 to the Pennsylvania State University. The authors thank William Winn and the anonymous reviewers for critical reading of this paper and for many useful comments and suggestions.

References

Agoris, D. P., V. P. Charalambakos, E. Pyrgloti, and S. Grzybowski (2004), A computational approach on the study of Franklin rod height impact on striking distance using a stochastic model, *J. Electrost.*, *60*(2–4), 175–181, doi:10.1016/j.elstat.2004.01.020.

Bazelyan, E. M., and Y. P. Raizer (1998), *Spark Discharge*, Chem. Rubber Co. Press, New York.

Bazelyan, E. M., and Y. P. Raizer (2000), *Lightning Physics and Lightning Protection*, Inst. of Phys. Publ. Ltd., Philadelphia, Pa.

Behnke, S. A., R. J. Thomas, P. R. Krehbiel, and W. Rison (2005), Initial leader velocities during intracloud lightning: Possible evidence for a runaway breakdown effect, *J. Geophys. Res.*, *110*, D10207, doi:10.1029/2004JD005312.

Coleman, L. M., T. C. Marshall, M. Stolzenburg, T. Hamlin, P. R. Krehbiel, W. Rison, and R. J. Thomas (2003), Effects of charge and electrostatic potential on lightning propagation, *J. Geophys. Res.*, *108*(D9), 4298, doi:10.1029/2002JD002718.

Dwyer, J. R. (2003), A fundamental limit on electric fields in air, *Geophys. Res. Lett.*, *30*(20), 2055, doi:10.1029/2003GL017781.

Femia, N., L. Niemeyer, and V. Tucci (1993), Fractal characteristics of electrical discharges: Experiments and simulation, *J. Phys. D Appl. Phys.*, *26*(4), 619–627, doi:10.1088/0022-3727/26/4/014.

Gallimberti, I., G. Bacchiega, A. Bondiou-Clergerie, and P. Lalande (2002), Fundamental processes in long air gap discharges, *C. R. Phys.*, *3*(10), 1335–1359, doi:10.1016/S1631-0705(02)01414-7.

Gurevich, A. V., and K. P. Zybin (2001), Runaway breakdown and electric discharges in thunderstorms, *Phys. Uspekhi*, *44*(11), 1119–1140.

Gurevich, A. V., G. M. Milikh, and R. A. Roussel-Dupré (1992), Runaway electron mechanism of air breakdown and preconditioning during a thunderstorm, *Phys. Lett. A.*, *165*(5)–(6), 463–468, doi:10.1016/0375-9601(92)90348-P.

Hager, W. W., J. S. Nisbet, J. R. Kasha, and W.-C. Shann (1989), Simulation of electric fields within a thundercloud, *J. Atmos. Sci.*, *46*(23), 3542–3558.

Helsdon, J. H., Jr., and K. Poeppel (2005), A 3D non grid-point-dependent lightning scheme, *Eos Trans. AGU*, *86*(52), Fall Meet. Suppl., Abstract AE41A-0147.

Helsdon, J. H., Jr., G. Wu, and R. D. Farley (1992), An intracloud lightning parameterization scheme for a storm electrification model, *J. Geophys. Res.*, *97*(D5), 5865–5884.

Helsdon, J. H., Jr., S. Gattaleeradapan, R. D. Farley, and C. C. Waits (2002), An examination of the convective charging hypothesis: Charge structure, electric fields, and Maxwell currents, *J. Geophys. Res.*, *107*(D22), 4630, doi:10.1029/2001JD001495.

Hockney, R., and J. Eastwood (1981), *Computer Simulation Using Particles*, McGraw-Hill, New York.

Kasemir, H. W. (1960), A contribution to the electrostatic theory of a lightning discharge, *J. Geophys. Res.*, *65*(7), 1873–1878.

Krehbiel, P. R. (1981), An analysis of the electric field change produced by lightning, Ph.D. thesis, Univ. of Manchester Inst. of Sci. and Technol., Manchester, U. K.

Krehbiel, P. R., M. Brook, S. Khanna-Gupta, C. Lennon, and R. Lhermitte (1984a), Some results concerning VHF lightning radiation from the real-time LDAR system at KSC, Florida, paper presented at VIIth International Conference on Atmospheric Electricity, Am. Meteorol. Soc., Albany, N. Y.

Krehbiel, P. R., R. Tennis, M. Brook, E. W. Holmes, and R. Comes (1984b), A comparative study of the initial sequence of lightning in a small Florida thunderstorm, paper presented at VIIth International Conference on Atmospheric Electricity, Am. Meteorol. Soc., Albany, N. Y.

Krehbiel, P., W. Rison, R. Thomas, T. Marshall, M. Stolzenburg, W. Winn, and S. Hunyady (2004), Thunderstorm charge studies using a simple cylindrical charge model, electric field measurements, and lightning mapping observations, *Eos Trans. AGU*, *85*(47), Fall Meet. Suppl., Abstract AE23A-0843.

Kupershtokh, A. L., V. Charalambakos, D. Agoris, and D. I. Karpov (2001), Simulation of breakdown in air using cellular automata with streamer to leader transition, *J. Phys. D Appl. Phys.*, *34*(6), 936–946, doi:10.1088/0022-3727/34/6/315.

Lehtinen, N. G., T. F. Bell, and U. S. Inan (1999), Monte Carlo simulation of runaway MeV electron breakdown with application to red sprites and terrestrial gamma ray flashes, *J. Geophys. Res.*, *104*(A11), 24,699–24,712.

Liu, N., and V. P. Pasko (2006), Effects of photoionization on similarity properties of streamers at various pressures in air, *J. Phys. D Appl. Phys.*, *39*, 327–334, doi:10.1088/0022-3727/39/2/013.

Liu, X. S., and P. R. Krehbiel (1985), The initial streamer of intracloud lightning flashes, *J. Geophys. Res.*, *90*(D4), 6211–6218.

MacGorman, D. R., J. M. Straka, and C. L. Ziegler (2001), A lightning parameterization for numerical cloud models, *J. Appl. Meteorol.*, *40*(3), 459–478.

Mansell, E. R., D. R. MacGorman, C. L. Ziegler, and J. M. Straka (2002), Simulated three-dimensional branched lightning in a numerical thunderstorm model, *J. Geophys. Res.*, *107*(D9), 4075, doi:10.1029/2000JD000244.

Mansell, E. R., D. R. MacGorman, C. L. Ziegler, and J. M. Straka (2005), Charge structure and lightning sensitivity in a simulated multicell thunderstorm, *J. Geophys. Res.*, *110*, D12101, doi:10.1029/2004JD005287.

Marshall, T. C., M. P. McCarthy, and W. D. Rust (1995), Electric field magnitudes and lightning initiation in thunderstorms, *J. Geophys. Res.*, *100*(D4), 7097–7104.

Marshall, T. C., M. Stolzenburg, C. R. Maggio, L. M. Coleman, P. R. Krehbiel, T. Hamlin, R. J. Thomas, and W. Rison (2005), Observed electric fields associated with lightning initiation, *Geophys. Res. Lett.*, *32*(3), L03813, doi:10.1029/2004GL021802.

Mazur, V., and L. H. Ruhnke (1998), Model of electric charges in thunderstorms and associated lightning, *J. Geophys. Res.*, *103*(D18), 23,299–23,308.

McCarthy, M. P., and G. K. Parks (1992), On the modulation of X-ray fluxes in thunderstorms, *J. Geophys. Res.*, *97*(D5), 5857–5864.

Niemeyer, L., and H. J. Wiesmann (1987), Modeling of leader branching in electronegative gases, in *Gaseous Dielectrics V: Proceedings of the Fifth International Symposium on Gaseous Dielectrics: Knoxville, TN, 3–7 May*, pp. 134–139, Pergamon, New York.

Niemeyer, L., L. Pietrono, and H. J. Wiesmann (1984), Fractal dimension of dielectric breakdown, *Phys. Rev. Lett.*, *52*(12), 1033–1036, doi:10.1103/PhysRevLett.52.1033.

Niemeyer, L., L. Pietrono, and H. J. Wiesmann (1986), Fractal dimension of dielectric breakdown—Response, *Phys. Rev. Lett.*, *57*(5), 650, doi:10.1103/PhysRevLett.57.650.

Niemeyer, L., L. Ullrich, and N. Wiegart (1989), The mechanism of leader breakdown in electronegative gases, *IEEE Trans. Electr. Insul.*, *24*(2), 309–324, doi:10.1109/14.90289.

Ogawa, T., and M. Brook (1964), Mechanism of intracloud lightning discharge, *J. Geophys. Res.*, *69*(24), 5141–5150.

Pasko, V. P. (2006), Theoretical modeling of sprites and jets, in *Sprites, Elves and Intense Lightning Discharges*, *NATO Sci. Ser. II: Mathematics, Physics and Chemistry*, vol. 225, edited by M. Füllekrug, E. A. Mareev, and M. J. Rycroft, pp. 253–311, Springer, Heidleberg, Germany.

Pasko, V. P., and J. J. George (2002), Three-dimensional modeling of blue jets and blue starters, *J. Geophys. Res.*, *107*(A12), 1458, doi:10.1029/2002JA009473.

Pasko, V. P., U. S. Inan, and T. F. Bell (2000), Fractal structure of sprites, *Geophys. Res. Lett.*, *27*(4), 497–500.

Pasko, V. P., U. S. Inan, and T. F. Bell (2001), Mesosphere-troposphere coupling due to sprites, *Geophys. Res. Lett.*, *28*(19), 3821–3824.

Petrov, N. I., and G. N. Petrova (1993), Physical mechanisms for intracloud lightning discharges, *Techn. Phys.*, *38*(4), 287–290.

Petrov, N. I., G. N. Petrova, and F. D'Alessandro (2003), Quantification of the probability of lightning strikes to structures using a fractal approach, *IEEE Trans. Dielectr. Electr. Insul.*, *10*(4), 641–654, doi:10.1109/TDEI.2003.1219649.

Poeppel, K. (2005), A 3D Lightning parameterization with branching and charge induction, Master's thesis, S. D. Sch. of Mines and Technol., Rapid City.

Popov, N. A. (2002), Spatial structure of the branching streamer channel in a corona discharge, *Plasma Phys. Rep.*, *28*(7), 615–622, doi:10.1134/1.1494061.

Press, W. H., B. P. Flannery, S. A. Teukolsky, and W. T. Vetterling (1992), *Numerical Recipes in C: The Art of Scientific Computing*, 2nd ed., Cambridge Univ. Press, New York.

Proctor, D. E. (1981), VHF radio pictures of cloud flashes, *J. Geophys. Res.*, *86*(C5), 4041–4071.

Proctor, D. E. (1983), Lightning and precipitation in a small multicellular thunderstorm, *J. Geophys. Res.*, *88*(C9), 5421–5440.

Proctor, D. E. (1997), Lightning flashes with high origins, *J. Geophys. Res.*, *102*(D2), 1693–1706.

Raizer, Y. P. (1991), *Gas Discharge Physics*, Springer, New York.

Rakov, V. A., and M. A. Uman (2003), *Lightning: Physics and Effects*, Cambridge Univ. Press, New York.

Riousset, J. A. (2006), Fractal modeling of lightning discharges, Master's thesis, Pa. State Univ., University Park.

Riousset, J. A., V. P. Pasko, P. R. Krehbiel, R. J. Thomas, and W. Rison (2006), Three-dimensional fractal modeling of intracloud lighting discharge in a New Mexico thunderstorm and comparison with lightning mapping observations, *Eos Trans. AGU*, *87*(52), Fall Meet. Suppl., Abstract AE21A-0996.

Rison, W., R. J. Thomas, P. R. Krehbiel, T. Hamlin, and J. Harlin (1999), A GPS-based three-dimensional lightning mapping system: Initial observations in central New Mexico, *Geophys. Res. Lett.*, *26*(23), 3573–3576.

Roussel-Dupré, R. A., A. V. Gurevich, T. Tunnel, and G. M. Milikh (1994), Kinetic theory of runaway breakdown, *Phys. Rev. E*, *49*(3), 2257–2271, doi:10.1103/PhysRevE.49.2257.

Rust, W. D., and T. C. Marshall (1996), On abandoning the thunderstorm tripole-charge paradigm, *J. Geophys. Res.*, *101*(D18), 23,499–23,504.

Rust, W. D., D. R. MacGorman, E. C. Bruning, S. A. Weiss, P. R. Krehbiel, R. J. Thomas, W. Rison, T. Hamlin, and J. Harlin (2005), Inverted-polarity electrical structures in thunderstorms in the severe thunderstorm electrification and precipitation study (STEPS), *Atmos. Res.*, *76*(1–4), 247–271.

Satpathy, S. (1986), Fractal dimension of dielectric breakdown—Comment, *Phys. Rev. Lett.*, *57*(5), 649, doi:10.1103/PhysRevLett.57.649.

Shao, X. M., and P. R. Krehbiel (1996), The spatial and temporal development of intracloud lightning, *J. Geophys. Res.*, *101*(D21), 26,641–26,668.

Shao, X. M., M. Stanley, P. R. Krehbiel, W. Rison, G. Gray, and V. Mazur (1996), Results of observations with the New Mexico Tech lightning interferometer, paper presented at Xth International Conference on Atmospheric Electricity, Int. Comm. on Atmos. Electr., Osaka, Japan.

Stolzenburg, M., W. D. Rust, and T. C. Marshall (1998), Electrical structure in thunderstorm convective regions: 3. Synthesis, *J. Geophys. Res.*, *103*(D12), 14,097–14,108.

Stolzenburg, M., T. C. Marshall, W. D. Rust, E. Bruning, D. R. MacGorman, and T. Hamlin (2007), Electric field values observed near lightning flash initiations, *Geophys. Res. Lett.*, *34*(4), L04804, doi:10.1029/2006GL028777.

Uman, M. A. (1984), *Lightning*, reprint ed., Dover, Mineola, N. Y.

Uman, M. A. (2001), *The Lightning Discharge*, Dover, Mineola, N. Y.

Vonnegut, B. (1983), Deductions concerning accumulations of electrified particles in thunderclouds based on electric field changes associated with lightning, *J. Geophys. Res.*, *88*(C6), 3911–3912.

Wiesmann, H. J., and H. R. Zeller (1986), A fractal model of dielectric breakdown and prebreakdown in solid dielectrics, *J. Appl. Phys.*, *60*(5), 1770–1773, doi:10.1063/1.337219.

Williams, E. R. (1989), The tripolar structure of thunderstorms, *J. Geophys. Res.*, *94*(D11), 13,151–13,167.

Williams, E. R., C. M. Cooke, and K. A. Wright (1985), Electrical discharge propagation in and around space charge clouds, *J. Geophys. Res.*, *90*(D4), 6059–6070.

Winn, W. P., and L. G. Byerley III (1975), Electric field growth in thunderclouds, *Q. J. R. Meteorol. Soc.*, *101*, 979–994.

Zahn, M. (1987), *Electromagnetic Field Theory: A Problem Solving Approach*, reprint ed., Krieger, Melbourne, Fla.

Ziegler, C. L., and D. R. MacGorman (1994), Observed lightning morphology relative to modeled space charge and electric field distributions in a tornadic storm, *J. Appl. Meteorol.*, *51*(6), 833–851.

P. R. Krehbiel, Physics Department, New Mexico Institute of Mining and Technology, Socorro, NM 87801, USA. (krehbiel@ibis.nmt.edu)

V. P. Pasko and J. A. Riousset, Communications and Space Sciences Laboratory, Department of Electrical Engineering, Pennsylvania State University, 211B Electrical Engineering East, University Park, PA 16802, USA. (vpasko@psu.edu; jar471@psu.edu)

W. Rison and R. J. Thomas, Electrical Engineering Department, New Mexico Institute of Mining and Technology, Socorro, NM 87801, USA. (rison@ee.nmt.edu; thomas@nmt.edu)